Cessations and reversals of the large-scale circulation in turbulent thermal convection

Heng-Dong Xi and Ke-Qing Xia
Department of Physics, The Chinese University of Hong Kong, Shatin, Hong Kong, China
(Received 15 December 2006; published 8 June 2007)

We present an experimental study of cessations and reversals of the large-scale circulation (LSC) in turbulent thermal convection in a cylindrical cell of aspect ratio (Γ) 1/2. It is found that cessations and reversals of the LSC occur in $\Gamma=1/2$ geometry an order-of-magnitude more frequently than they do in $\Gamma=1$ cells, and that after a cessation the LSC is most likely to restart in the opposite direction, i.e., reversals of the LSC are the most probable cessation events. This contrasts sharply to the finding in $\Gamma=1$ geometry and implies that cessations in the two geometries are governed by different dynamics. It is found that the occurrence of reversals is a Poisson process and that a stronger rebound of the flow strength after a reversal or cessation leads to a longer period of stability of the LSC. Several properties of reversals and cessations in this system are found to be statistically similar to those of geomagnetic reversals. A direct measurement of the velocity field reveals that a cessation corresponds to a momentary decoherence of the LSC.

DOI: 10.1103/PhysRevE.75.066307 PACS number(s): 47.27.−i, 05.65.+b, 47.55.P−, 91.25.Mf

Turbulent Rayleigh-Bénard (RB) convection has proven to be a fruitful paradigm for studying buoyancy-driven turbulent flows that occur ubiquitously in nature. At sufficiently high values of the Rayleigh number, Ra, a large-scale circulation (LSC) also known as the mean wind of turbulent convection, in the form of a single roll comparable to the size of the convection cell, emerges [1–7]. An intriguing dynamic feature of the LSC is the apparently erratic orientational change of its nearly vertical circulation plane [8–14]. This change arises either as a result of the azimuthal motion of the LSC with no significant reduction of its flow strength, or as a result of the LSC starting in a new orientation after a momentary vanishing of its flow strength, i.e., a cessation of the LSC [12–14]. The azimuthal motion is Brownian in character over short time scales but generates net rotations over longer time scales [11–14]. Cessations that lead to a 180° change of the LSC's orientation correspond to a reversal of its flow direction. Reversals have been observed in two-dimensional numerical simulations [15] and are the subject of recent model studies [10,16–18]. In addition to its importance in understanding the dynamics of turbulent flows in the RB system, the putative connection of this phenomenon to similar reversals in the magnetic polarity of the Earth [19] and in the wind direction in the Earth's atmosphere [20] also makes it of more general interest. For example, flow reversals were also observed in two-dimensional turbulence [21], and an analogy has been made between the reversal phenomenon and the behavior of condensed matter systems near criticality [22]. However, because earlier experiments cannot unambiguously distinguish cessation-led reversals from those caused by azimuthal rotations [9,10] and because of the extremely low probability of occurrence of cessation-led reversals [12–14], detailed statistical analysis of unambiguously identified cessation-led reversal events has not been possible.

A common feature of the existing experimental studies of reversals and cessations is that they were all conducted in an aspect ratio ($\Gamma=D/H$) unity cylindrical cell, where D is the diameter and H the height of the cell. Most theoretical studies [10,16,17] that aim to model the reversal phenomenon also assume $\Gamma=1$ geometry either explicitly or implicitly [23]. One would therefore naturally ask whether cessations occur in cells with geometry other than $\Gamma=1$. In this paper, we report experimental studies of cessations and reversals in a $\Gamma=1/2$ cylindrical cell, using water as the convecting fluid. The convection cell consists of top and bottom copper plates of thickness 1 cm and a sidewall made of a Plexiglas tube of inner diameter 19 cm and wall thickness 5 mm. Its other details have been described in [24,25]. In all measurements the cell was leveled to within 0.06°. The method used for measuring the azimuthal orientation and strength of the LSC is similar to that used in [12,14] for $\Gamma=1$ cells. The technique takes advantage of the fact that the LSC is essentially an organized flow of thermal plumes [6] and that when it flows up (down) along the sidewall, it carries hot (cold) fluid. Therefore, by measuring the relative temperature differences along the perimeter of the sidewall, the orientation and strength of the LSC may be obtained. In order for this method to be applicable to $\Gamma=1/2$ cells, the overall flow should be a single circulating roll. Flow in the $\Gamma=1/2$ geometry has been studied in local velocity measurements and numerical simulations [4,26,27], and it is found that overall LSC in this cell has a single-roll structure, which is shown to be the case in a recent direct measurement of the velocity field [11]. In the present case, 24 thermistors are placed in blind holes that are drilled from the outside into the sidewall of the convection cell. These holes are distributed in three horizontal rows at heights $H/4$, $H/2$, and $3H/4$ and in eight vertical columns equally spaced azimuthally around the cylinder and their ends have a distance of 0.7 mm from the convecting fluid. The thermistors have a diameter of 2.5 mm with a time constant of 1 s (Omega, 44031) and are calibrated individually with an accuracy of 0.01 °C. They are connected to a multichannel multimeter and their resistances are measured at a sampling frequency of 0.29 Hz, which are then converted into temperatures. By fitting the function [12] $T_i=T_0+A\cos(i\pi/4-\phi)$, $i=0,\ldots,7$, separately at each time step, to the eight temperatures in one row, we obtain the amplitude A, which is a measure of the strength, or magnitude, of the LSC, and ϕ, which give the azimuthal orienta-

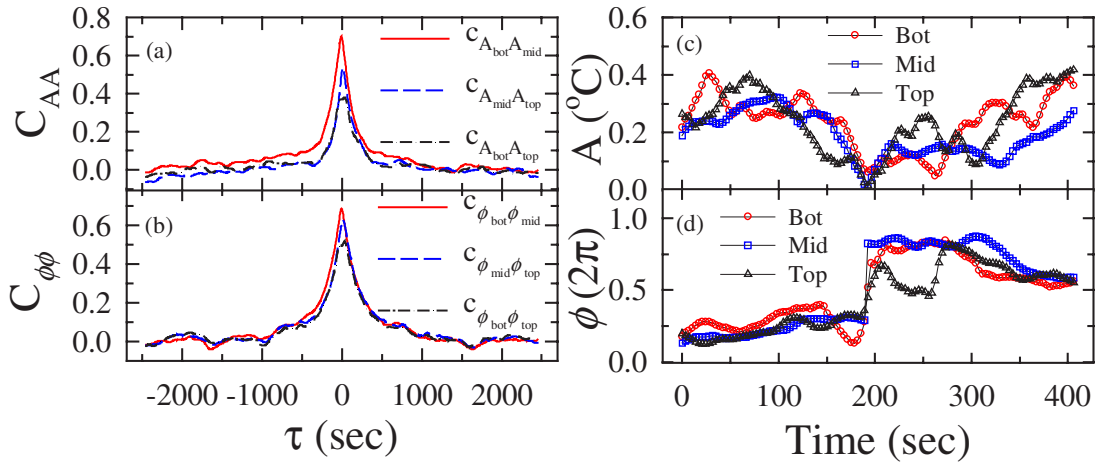

FIG. 1. (Color online) (a) Cross-correlation functions between the amplitude trace A measured at different heights. (b) Similar to those of (a) but for the angular trace ϕ. (c) An example illustrating a global cessation of the LSC, in which flow strength A of the LSC measured at the three heights experiences a simultaneous momentary vanishing. (d) Corresponding time trace of ϕ, showing that the orientation of the LSC restarts in the opposite direction after the global cessation.

tion of the LSC (the angular position at which the hot fluid comes up). The typical error of the fitting is 16% for A and 13° for ϕ.

Measurements, each lasting at least 2 days, were made with Ra varying from 1.5×10^{10} to 7.2×10^{10} and with the Prandtl number Pr varying from 4.9 to 5.3. In addition, an extra-long measurement lasting 34 days was made at Ra $=5.6\times10^{10}$ and Pr=5.0. Figures 1(a) and 1(b) plot, respectively, the cross-correlation functions $C_{AA}(\tau)$ between the amplitudes A, and $C_{\phi\phi}(\tau)$ between the angles ϕ, obtained at different heights from the 34-day measurement. The high level of correlation between ϕ, and between A, at different heights shows clearly that overall the LSC is a single-circulating roll that moves azimuthally as a whole throughout the height of the cell. The properties revealed by the time series of ϕ are similar to those observed in [11], obtained by placing a flow-indicator in the fluid, that the azimuthal motion of the LSC is erratic over short time scales and over a long time it generates a net rotation. It was found in [11] that the short-time behavior of ϕ is Brownian in character. Here we focus on events that involve the momentary vanishing of the magnitude of the LSC, i.e., cessations. One such example is shown in Fig. 1(c) for A measured at the three heights, with Fig. 1(d) showing the corresponding ϕ. These results show that a momentary vanishing of the flow strength of the LSC occurs simultaneously throughout the height of the cell, accompanied by a change of ϕ of approximately 180°, i.e., the aspect-ratio-one-half single circulating roll has experienced a "global cessation" and then restarts in the opposite direction. Operationally, we identify a cessation event whenever A is below a threshold A_c. Values of A_c ranging from $0.05\langle A\rangle$ to $0.3\langle A\rangle$ have been tried and the identified cessations all give qualitatively the same statistical behavior. For the results presented below, we used $A_c=0.15\langle A\rangle$, which is the same as that used in [14]. We have identified 1813, 1855, and 1798 cessation events from the 34-day data for the top, middle, and bottom rows of thermistors, respectively. It is found that the cessations and reversals measured at different Ra have the same statistical properties. Unless stated otherwise, all the statistical results presently below will be based on the 34-day data and most of them will come from the middle row thermistors.

We now examine the orientational change $\Delta\phi$ of the LSC after a cessation. Figure 2(a) shows the PDF (probability density function) $P(\Delta\phi)$ from the 34-day data for the top, middle, and bottom row of thermistors, respectively. It is seen that all three data sets show consistently that $|\Delta\phi|=180°$ is the most probable angular change for the orientation of the LSC, i.e., after a cessation the LSC is most likely to restart in the opposite direction. This is the reversal that is the subject in some of the recent theoretical models [10,16–18]. Note that the present result contrasts sharply to the uniform distribution of $\Delta\phi$ found for $\Gamma=1$ cells [12–14], which implies that the dynamics governing cessations are different in the two geometries. A uniform distribution implies that the system has lost its memory during the cessation and the LSC is equally likely to restart in any orientation. Whereas the nonuniform distribution shows the system has certain memory.

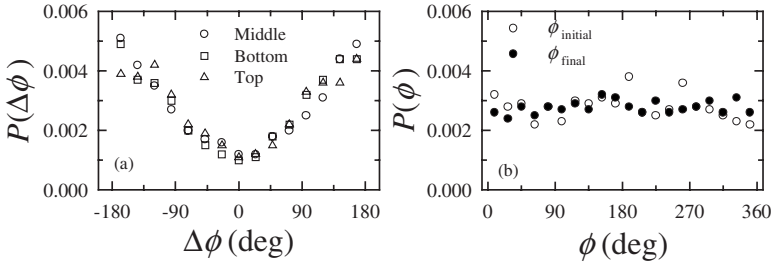

FIG. 2. (a) PDFs of the LSC's orientational angular change $\Delta\phi$ after a cessation measured at the three heights, respectively. (b) PDFs of the angle $\phi_{initial}$ at the start and the angle ϕ_{final} at the end of a cessation.

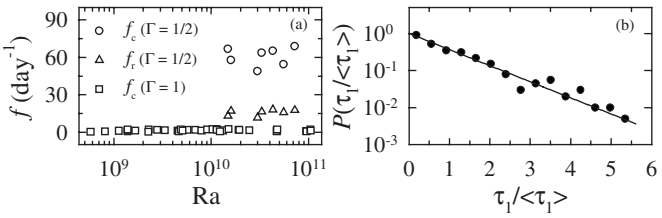

FIG. 3. (a) Cessation and reversal frequencies f_c and f_r vs Ra and comparison between the $\Gamma=1/2$ and 1 (from Ref. [14]) results. (b) PDF of the time interval t_1 between successive reversals.

In Fig. 2(b) we show the PDF of $\phi_{initial}$, the orientational angle of LSC at the start of a cessation, and that of ϕ_{final}, the angle at the end of a cessation. The essentially uniform distributions of $\phi_{initial}$ and ϕ_{final} suggest that there is no systematic bias in the apparatus and measurements, i.e., a cessation event is likely to start and, to end, at any angle. This finding is also consistent with that found in the $\Gamma=1$ geometry [14]. We define reversal events among cessations as those with $|\Delta\phi| \geqslant 150°$, since the LSC may be considered to have reversed its orientation when $|\Delta\phi|$ is over this value. A total of 543 reversals are identified from the 1855 cessations, and the $\phi_{initial}$ and ϕ_{final} for these are also found to have uniform distributions. Figure 3(a) plots the cessation and reversal frequencies f_c and f_r as functions of Ra, respectively. It is seen that on average $f_c \approx 60/\text{day}$ and $f_r \approx 16/\text{day}$. Also shown in the figure is f_c obtained in $\Gamma=1$ cells [14], which has an average value of $\approx 1.5/\text{day}$. The apparent Ra independence of f_c and f_r in $\Gamma=1/2$ geometry is consistent with the result for cessations found in $\Gamma=1$ cells [12–14]. A quantity of interest is the time interval between successive cessations or reversals, which we denote as t_1. Figure 3(b) shows, on a semilog scale, the PDF $P(t_1/\langle t_1\rangle)$ of the normalized $t_1/\langle t_1\rangle$ obtained from the 543 reversals, where the average value $\langle t_1\rangle = 89.4$ min. The solid line represents the function $P(t_1/\langle t_1\rangle)=\exp(-t_1/\langle t_1\rangle)$. It is found that t_1 based on the 1855 cessations also exhibits an exponential distribution, with $\langle t_1\rangle = 26.3$ min. These results suggest that both cessations and reversals obey a Poisson process, i.e., successive cessation or reversal events are independent of each other. Exponential distribution of t_1 has been observed in the $\Gamma=1$ case [14] for cessations. Figure 3 represents the first such result for purely reversal events, which is consistent with a recent theoretical result [16].

Next we analyze the statistical properties of flow intensity change and related time scales during cessations or reversals. Denote A_d as the local maximum of A preceding a cessation or reversal and A_{min} the minimum value of A reached in the cessation or reversal, the normalized "decline amplitude" is then defined as $\delta A_d=(A_d-A_{min})/\langle A\rangle$. The normalized "rebound amplitude" is similarly defined as $\delta A_r=(A_r-A_{min})/\langle A\rangle$, where A_r is the local maximum of A after it rebounds from A_{min}. The decline time t_d is defined as the time interval between A_d and A_{min}, and the rebound time t_r the time interval between A_{min} and A_r. The reversal time t_{rev} is defined as the time interval during which a 180° change of ϕ takes place. Operationally t_{rev} is determined as the time interval in which $|d\phi/dt|$ is larger than a threshold (here chosen to be $8\langle|d\phi/dt|\rangle$) *within* a cessation. Figure 4(a) plots the PDFs of δA_d and δA_r for the 543 reversals. In Fig. 4(b) we show for reversals the PDFs of the normalized t_d/T_c, t_r/T_c, and t_{rev}/T_c, where T_c is the circulation time of the LSC, which is taken to be $(2H+2D)/\langle V\rangle$. Using previously measured average velocity $\langle V\rangle$ of the LSC [11,28], we obtain $T_c=150$ s for the present Ra. For cessations the above quantities are found to exhibit similar properties as those shown in Figs. 4(a) and 4(b). These results show that the decline part of a reversal is generally deeper and lasts longer than the rebound part ($\langle\delta A_d\rangle/\langle\delta A_r\rangle=0.90/0.53$). This suggests that in general it will take several rebounds for the flow strength to recover to its level before cessation. Figure 4(b) also shows that the reversal process in terms of the orientational angular change is very short as compared to the relatively long decline and rebound time scales, the average reversal interval $\langle t_{rev}\rangle=0.1T_c$ as compared to $\langle t_d\rangle=0.5T_c$ and $\langle t_r\rangle=0.3T_c$. It is also found that, on average, the "reversal process" (or change of ϕ) does not begin until the flow strength has declined 90% of the previous maximum. The relationship of the amplitude of rebound δA_r and the interval t_1 between cessations or reversals may be studied by the normalized cross-correlation: $C_{\delta A_r t_1}(n)=\langle[\delta A_r(i+n)-\langle\delta A_r\rangle][t_1(i)-\langle t_1\rangle]\rangle/\sigma_{\delta A_r}\sigma_{t_1}$, where i and n denote the individual events and $\sigma_{\delta A_r}$ and σ_{t_1} are the standard deviations of the two quantities, respectively. In

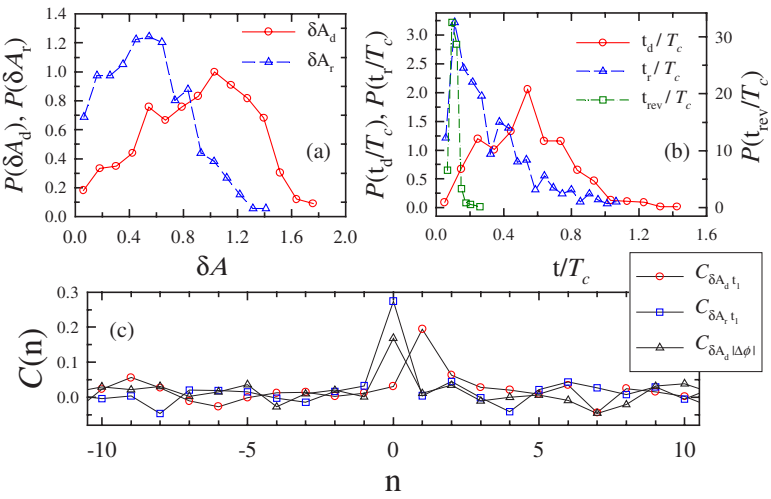

FIG. 4. (Color online) PDFs of the normalized (a) decline and rebound amplitudes δA_d and δA_r and (b) decline and rebound times t_d/T_c and t_r/T_c, all for reversal events. Also shown in (b) is the PDF of the normalized reversal time t_{rev}/T_c. (c) Cross-correlation functions between δA_d and t_1, δA_r and t_1, and δA_d and $|\Delta\phi|$, respectively.

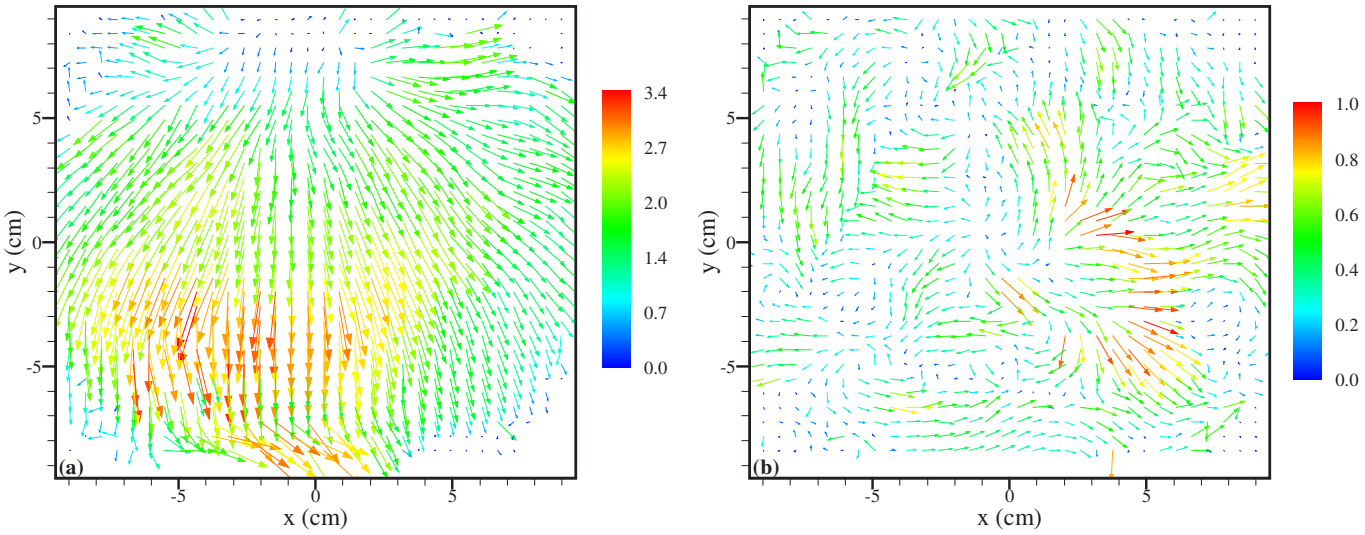

FIG. 5. (Color online) Snapshots of the two-dimensional horizontal velocity field (in cm/s) measured 1 cm below the top plate of the convection cell showing (a) a coherent LSC and (b) decoherence of the LSC during cessation.

Fig. 4(c) we plot $C_{\delta A_r t_1}(n)$. The positive correlation between δA_r and the immediately following t_1 implies that a stronger rebound of flow strength after a reversal or cessation leads to a longer time period of no reversals or cessations, i.e., the stability of LSC depends on the rebound strength.

Also plotted in Fig. 4 are cross-correlation functions of δA_d and t_1 and of δA_d and $|\Delta\phi|$. The positive peak of $C_{\delta A_d t_1}(n)$ at $n=1$ indicates that a large t_1 is likely to produce a deep decline of the flow strength in the *next* cessation or reversal. The positive peak of $C_{\delta A_d|\Delta\phi|}(n)$ at $n=0$ shows that a deep decline is likely to result in a larger orientational change in a cessation event. It is interesting to note that the statistical properties of the decline and rebound amplitudes and the associated time scales shown in Fig. 4 are qualitatively similar to certain features of the geomagnetic field during its polarity reversals. For example, it has been found from paleomagnetic records that the field intensity underwent a long decline preceding a polarity reversal that was followed by a rapid rebound of the intensity afterwards [29]. Paleomagnetic records also revealed that a large rebound of the field intensity after a reversal usually results in a longer period of time without reversals. The time interval between geomagnetic reversals is found to also exhibit an exponential distribution [30]. Obviously the simple system of Rayleigh-Bénard convection and the convective flow of the Earth's outer core differ in many ways, but if the idealized RB system is able to capture some essential features that are common to the phenomena of flow reversals occurring in a wide variety of systems, then detailed statistical analysis of the reversal phenomenon in this system may shed some light on reversals in more complicated systems such as convection in the Earth's outer core.

It is seen that during a cessation the flow strength of the LSC vanishes momentarily, as measured by A. A natural question is what actually happens to the flow field. This may be answered by direct measurement of the velocity field using the particle image velocimetry (PIV) technique. To do this, a cell with a top plate made of sapphire was used. Details of the cell and the PIV measurement have been described in Ref. [13]. The only differences are that in [13] the aspect ratio is 1 and that here the measuring area, containing 709 velocity vectors, covers the whole horizontal cross section of the cell. Figure 5 shows two instantaneous 2D horizontal velocity fields, (a) the LSC is in a "normal" state and (b) it is undergoing a cessation. It is seen that most of the individual velocity vectors are aligned largely in the same direction in the normal state, giving rise to a coherent LSC; whereas the flow field appears random during a cessation. A cessation may therefore be understood as a momentary decoherence of the LSC. This physical picture gives insight into the mechanism of cessations and reversals. We found that for the $\Gamma=1$ case a cessation also corresponds to a decoherence of the LSC.

In summary, our experiment in an aspect-ratio 1/2 cylindrical convection cell shows that cessations of the large-scale circulation not only occur but do so an order of magnitude more frequently than they do in $\Gamma=1$ and that reversals of the LSC are the most probable events among cessations, again in sharp contrast to the uniform distribution of orientational change found in $\Gamma=1$ cells. This result suggests different cessation dynamics for the two geometries. It remains to be seen if the current models, when properly modified, are able to explain and reproduce the properties of reversals and cessations found in the present system.

This work was supported by the Research Grants Council of Hong Kong under Grant No. 403003 and 403705. We thank G. Ahlers and R. Benzi for helpful discussions. K. Q. X. gratefully acknowledges the support of the Croucher Foundation of Hong Kong.

[1] R. Krishnamurti and L. N. Howard, Proc. Natl. Acad. Sci. U.S.A. **78**, 1981 (1981).
[2] M. Sano, X.-Z. Wu, and A. Libchaber, Phys. Rev. A **40**, 6421 (1989).
[3] B. Castaing, G. Gunaratne, F. Heslot, L. Kadanoff, A. Libchaber, S. Thomae, X.-Z. Wu, S. Zaleski, and G. Zanetti, J. Fluid Mech. **204**, 1 (1989).
[4] X.-L. Qiu and P. Tong, Phys. Rev. E **64**, 036304 (2001).
[5] K.-Q. Xia, C. Sun, and S.-Q. Zhou, Phys. Rev. E **68**, 066303 (2003).
[6] H.-D. Xi, S. Lam, and K.-Q. Xia, J. Fluid Mech. **503**, 47 (2004).
[7] C. Sun, K.-Q. Xia, and P. Tong, Phys. Rev. E **72**, 026302 (2005a).
[8] S. Cioni, S. Ciliberto, and J. Sommeria, J. Fluid Mech. **335**, 111 (1997).
[9] J. J. Niemela, L. Skrbek, K. R. Sreenivasan, and R. J. Donnelly, J. Fluid Mech. **449**, 169 (2001).
[10] K. R. Sreenivasan, A. Bershadskii, and J. J. Niemela, Phys. Rev. E **65**, 056306 (2002).
[11] C. Sun, H.-D. Xi, and K.-Q. Xia, Phys. Rev. Lett. **95**, 074502 (2005b).
[12] E. Brown, A. Nikolaenko, and G. Ahlers, Phys. Rev. Lett. **95**, 084503 (2005).
[13] H.-D. Xi, Q. Zhou, and K.-Q. Xia, Phys. Rev. E **73**, 056312 (2006).
[14] E. Brown and G. Ahlers, J. Fluid Mech. **568**, 351 (2006).
[15] U. Hansen, D. A. Yuen, and S. E. Kroening, Geophys. Astrophys. Fluid Dyn. **63**, 67 (1992).
[16] R. Benzi, Phys. Rev. Lett. **95**, 024502 (2005); R. Benzi and R. Verzicco (unpublished).
[17] F. F. Araujo, S. Grossmann, and D. Lohse, Phys. Rev. Lett. **95**, 084502 (2005).
[18] E. Brown and G. Ahlers, Phys. Rev. Lett. **98**, 134501 (2007).
[19] G. A. Glatzmaier, R. S. Coe, L. Hongre, and P. H. Roberts, Nature (London) **401**, 885 (1999).
[20] E. van Doorn, B. Dhruva, K. Sreenivasan, and V. Cassella, Phys. Fluids **12**, 1529 (2000).
[21] J. Sommeria, J. Fluid Mech. **170**, 139 (1986).
[22] R. C. Hwa, C. B. Yang, S. Bershadskii, J. J. Niemela, and K. R. Sreenivasan, Phys. Rev. E **72**, 066308 (2005).
[23] According to its authors, the model presented in [18], although applied to the unity aspect ratio case, may in principle be adapted to other aspect ratios.
[24] S.-L. Lui and K.-Q. Xia, Phys. Rev. E **57**, 5494 (1998).
[25] S.-Q. Zhou and K.-Q. Xia, Phys. Rev. E **63**, 046308 (2001).
[26] G. Stringano and R. Verzicco, J. Fluid Mech. **548**, 1 (2006).
[27] Y. Tsuji, T. Mizuno, T. Mashiko, and M. Sano, Phys. Rev. Lett. **94**, 034501 (2005).
[28] Y.-B. Xin and K.-Q. Xia, Phys. Rev. E **56**, 3010 (1997).
[29] J. P. Valet and L. Meynadier, Nature (London) **366**, 234 (1993).
[30] J. A. Jacobs, *Reversals of the Earth's Magnetic Field* (Cambridge University Press, New York, 1994).